

## Model predictive control stabilization of a power system including a wind power plant

Islam Ahmed Ali

Cairo University, Electrical Power Engineering Department, Giza, Egypt, islam.ali94@alumni.eng.cu.edu.eg

Abdel Latif Elshafei

Cairo University, Electrical Power Engineering Department, Giza, Egypt, elshafei@eng.cu.edu.eg

Submitted: 18.09.2021

Accepted: 19.03.2022

Published: 30.06.2022



**Abstract:** The conventional generators are equipped with power system stabilizers (PSS) to damp oscillations that follow disturbances. The inclusion of renewable energy sources within the existing power systems requires further investigations to enhance the performance of PSS. Several control strategies have been being used to design the PSS. In this paper, model predictive control (MPC) is investigated to be used as a PSS. It uses numerical optimization algorithms to get an optimal control output considering the system's constraints. Therefore, It is designed and applied to a multi-machine power system with a wind power plant (WPP). Three disturbances are used to test the controllers including three-phase fault, transmission line outage, and voltage reference sudden change. MATLAB/SIMULINK is used in the simulation. Then, the results are compared to conventional multi-band controller (MB) and linear quadratic regulator (LQR). MPC shows efficient performance in handling the constraints and damping types of oscillations with the existence of the WPP in the case of partial power-sharing.

**Keywords:** *Linear quadratic regulator, Model predictive control, Power system stabilizer, State feedback control, Wind power plant*

Cite this paper as: Ali, I. A., & Elshafei, A. L., Model predictive control stabilization of a power system including a wind power plant. *Journal of Energy Systems* 2022; 6(2): 188-208, DOI: 10.30521/jes.997307

© 2022 Published by peer-reviewed open access scientific journal, JES at DergiPark (<https://dergipark.org.tr/en/pub/jes>)

| Nomenclature | Description                                       | Symbols        | Description   |
|--------------|---|----------------|---|
| AC           | Alternating Current                               | $V_{DC}$       | DC link voltage.                                    |
| AVR          | Automatic Voltage Regulator                       | $V_{DC,ref}$   | DC link voltage reference                           |
| MPC          | Model Predictive Control                          | $V_{t,abc}$    | terminal voltage in abc frame                       |
| DC           | Direct Current                                    | $V_{g,dq}$     | grid voltage in dq frame                            |
| IEEE         | Institute of Electrical and Electronics Engineers | $P_w$          | wind-generated power                                |
| LMI          | Linear Matrix Inequality                          | $P_g$          | power delivered to the grid                         |
| LQR          | Linear Quadratic Regulator                        | $Q_g$          | reactive power delivered to the grid                |
| MB           | Multi-Band Control                                | $Q_{g,ref}$    | reactive power reference delivered to the grid      |
| MMPS         | Multi-Machine Power System                        | $i_{dq}$       | current delivered to the grid in dq frame           |
| MPC          | Model Predictive Control                          | $i_{dq,ref}$   | current reference delivered to the grid in dq frame |
| N4SID        | Subspace State Space System Identification        | $\theta_{pll}$ | phase-locked loop angle                             |
| PI           | Proportional Integral Controller                  | $m_{dq}$       | modulation signal in dq frame                       |
| PID          | Proportional Integral Derivative Controller       | $m_{dq}$       | modulation signal in abc frame                      |
| PLL          | Phase Locked Loop                                 | $E_t$          | terminal voltage of the machine                     |
| PSS          | Power System Stabilizer                           | $\omega$       | Angular frequency of the machine.                   |
| PV           | Photo Voltaic                                     | $u$            | Input signal.                                       |
| SFC          | State Feedback Control                            |                |   |
| WPP          | Wind Power Plant                                  |                |   |

## 1. INTRODUCTION

Worldwide, the installed wind-energy capacity reached 744 Gigawatts in 2020 [1] achieving a 12.5% rate of growth. The contribution of wind energy to the total power generated in a grid varies from one country to another. Many grids have had a target to generate 20% of their needs using renewable energy by the year 2020. These facts dictate a strong need to study the stability and performance of power networks that have partial generations coming from renewable resources such as wind farms. Our objective here is to consider a two-area power network that has both conventional and wind power generation. The network could, of course, suffer from different disturbances that lead to oscillations in the tie-line power. Traditionally, power system stabilizers (PSS) are used to damp the oscillations. However, because of the system nonlinearities and the saturation limits imposed on the excitation, classical power system stabilizers may not perform optimally. This motivates the use of model predictive control algorithms to implement power system stabilizers that can abide by the system's constraints.

Practically, PSS is designed based on classical techniques in the frequency domain. According to the IEEE Standards [2], PSS includes single-input compensators such as PSS1A, and dual-input compensators such as PSS2B, PSS3B, and PSS4B. The PSS2B, PSS3B, and PSS4B have been enhanced by PSS2C, PSS3C, and PSS4C, respectively [3]. The enhancement is achieved by adding output logic functions in the case of PSS2C and PSS3C which define threshold values for passing the PSS control signal. Enhancement is also done by adding a fourth lead-lag block in the case of PSS2C and adding a very low-frequency band in the case of PSS4C for fine adjustment of the power frequency. Advanced design algorithms such as adaptive control [4, 5], robust control [4, 6], and intelligent control [7, 8, 9] have been investigated for the design of power system stabilizers. The main criticism of PSS based on advanced control algorithms is that they do not take the system constraints explicitly into consideration. Linear matrix inequality (LMI) techniques can accommodate constraints [10], but they are not popular yet because of the underlying mathematics.

Inclusion of wind power plants to cover partial load demands of a power system impose new challenges that should be addressed by designers to ensure stability following disturbances and comply with the system constraints. The authors in [11] investigate the challenges of wind power integration to the electrical grids and possible solutions. Wind power plants reduce the generation costs and pollution emissions of the fuels. However, there are also some challenges related to; power system quality like harmonics, frequency and voltage variations, power generation management due to the unpredicted wind energy nature, and power system control like the voltage, frequency, active, and reactive power. The difficulty increases with the high penetration of wind energy to the grid because it reduces the inertia of the power system [12].

Predictive control emerges as a potential candidate to perform this task. Predictive controllers are currently strong competitors of the popular PID controllers in the industry. They are based on a clear intuition and can optimally accommodate constraints. This motivates us to propose predictive controllers as PSS for systems that combine traditional and renewable energy sources. The proposed algorithm uses a discrete-time model of the system to predict the future outputs over a specific prediction horizon. At every sampling instant, an optimization problem is solved over the prediction horizon to compute the control actions. According to the receding horizon policy, the first control action is executed. The whole optimization problem is repeated in the following sampling interval. This strategy allows us to handle input constraints such as the limits imposed on the excitation systems. We can also accommodate state constraints such as maximum allowable frequency deviations. Accordingly, researchers investigate MPC in different applications such as load frequency control [13], maximum wind-power generation [14], and wind-farm voltage control [15].

Therefore, to prove the effectiveness of model predictive control as an underlying strategy to design effective PSS, the power system model proposed by Kundur [16] is modified to include partial generation from a wind power plant. The objective of the PSS is to preserve stability and maintain the tie-line power and frequency at their rated values following disturbances. Sever scenarios such as a three-phase fault, a transmission line outage, and a voltage reference sudden change will be examined. The proposed PSS is compared to the conventional multi-band (MB) PSS and a linear quadratic regulator (LQR).

The paper is organized as follows: Section 2 describes the system. Section 3 demonstrates the system identification process to get the state-space model of the conventional machines. Section 4 demonstrates the model predictive control. Section 5 explains the power system stabilizer. Section 6 includes the results and discussion. Section 7 summarizes and concludes the paper.

## 2. SYSTEM DESCRIPTION

The system as shown in Fig. 1 is developed based on Kundur’s model [17] by the authors in Ref. [18], which consists of four conventional machines distributed into two areas, to study the performance of the PSS on the interarea oscillations. Each machine in this model is controlled by a governor, an AVR, and a PSS. A step-up transformer is installed to each machine to tie the two areas by two transmission lines (220Km length). The data of the machines of Kundur’s model are presented in Table 1.

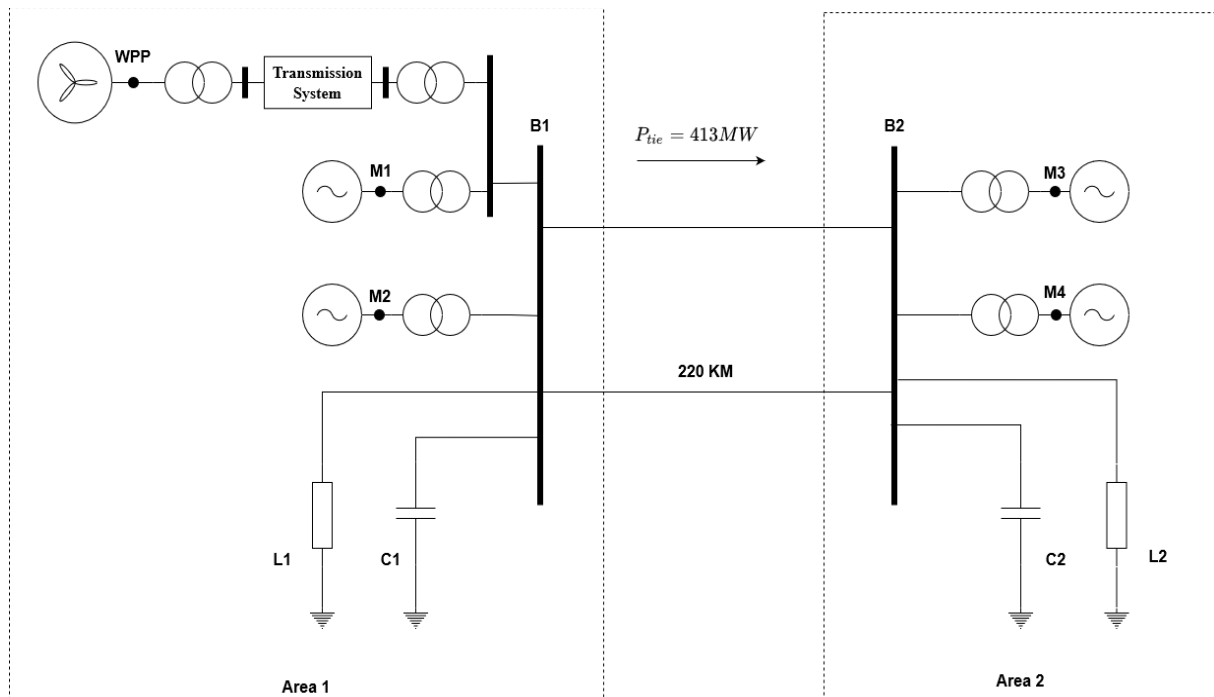


Figure 1. Schematic diagram of the system under study.

Table 1. Data of Kundur’s model machines.

|                    | Voltage (Kv) | Ratings     |                        |
|--------------------|--------------|-------------|------------------------|
|                    |              | Power (MVA) | Inertia Constant (sec) |
| Machines (M1 & M2) | 20           | 900         | 6.5                    |
| Machines (M3 & M4) | 20           | 900         | 6.175                  |
| Transformers       | 20/230       | 900         | -                      |

Each area has a constant impedance load and a capacitor bank installed to enhance the voltage profile to unity because the surging impedance loading of the transmission lines is around (140MVAR) for the single line. Their data are illustrated in Table 2.

Table 2. Data of the loads and capacitor banks.

|                     | MW   | MVAR       |
|---------------------|------|------------|
| Load (L1)           | 967  | 100 & -187 |
| Load (L2)           | 1767 | 100 & -187 |
| Capacitor Bank (C1) | -    | -200       |
| Capacitor Bank (C2) | -    | -350       |

A wind power plant (WPP) is installed in parallel to Machine (M1) via two step-up transformers and a transmission system to expand the model's function to study the performance of the PSS on the inter-area oscillations with the existence of the WPP. The data of the added machines are presented in Table 3.

Table 3. Data of the added machines.

|                                     | Ratings           |             |
|-------------------------------------|-------------------|-------------|
|                                     | Voltage (Kv)      | Power (MVA) |
| WPP                                 | 0.575             | 500         |
| Transformers (connected to the WPP) | 0.575/25 & 25/230 | 700         |

The WPP has many wind turbines generation Type 4 but in this model, it is modeled as an equivalent large generator with (500MVA) rating. This wind generation type consists of a wind turbine, synchronous generator, full-scale converter, filter, and controllers. The full-scale converter consists of a generator-side converter, DC link, and grid-side converter. The controller of the machine-side converter adjusts the active power and the stator voltage of the generator, meanwhile, that of the grid-side adjusts the DC link voltage and reactive power exchange with the grid. The existence of the full-scale converter and the DC link decouples the dynamics of the wind turbine from that of the grid. As a result, the used WPP model considers only the grid-side converter and its controllers. The components before the DC link are modeled as a power source obtained from the wind as presented in Fig. 2.

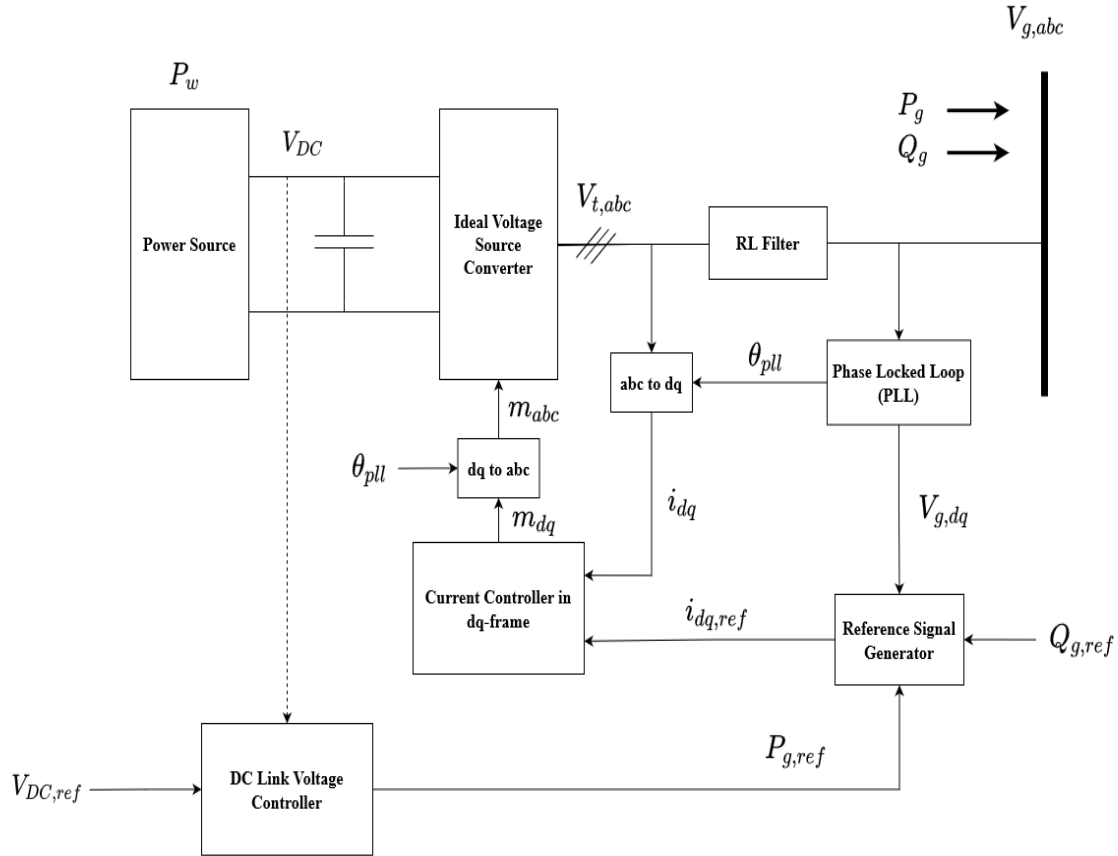


Figure 2. WPP block diagram

The grid-side converter uses three PI controllers for the DC link voltage, current, and AC voltage. The AC voltage is regulated to the reference value (1 pu) by controlling the reactive power. The DC link consists of only a capacitance. In addition, there is a filter consisting of resistance and inductance on the output of the converter as presented in Fig. 2. The data of the grid-side converter is illustrated in Table 4.

Table 4. Data of the WPP model.

|                                 | Components        |               |           |
|---------------------------------|-------------------|---------------|-----------|
|                                 | R ( $\mu\Omega$ ) | L ( $\mu H$ ) | C (mf)    |
| DC Link                         |                   |               | 760       |
| Filter                          | 11.9              | 1             |           |
| Grid-Side Converter Controllers |                   |               |           |
|                                 | P-gain            | I-gain        | Reference |
| DC Link Voltage                 | 500               | 500           | 1300VDC   |
| Current                         | 0.001             | 0.0119        |           |
| Reactive Power                  | 5                 | 5             | 1pu (VAC) |

The transmission system has some underground cables but it is modeled as an equivalent pi-model transmission line with the data presented in Table 5.

Table 5. Data of the transmission system.

|                            | Positive-Sequence                | Zero-Sequence                   | Line Length (Km) |
|----------------------------|----------------------------------|---------------------------------|------------------|
| Resistance ( $\Omega/Km$ ) | 0.1153/100                       | 0.413/100                       |                  |
| Inductance ( $H/Km$ )      | $1.05 \times 10^{-3}/50$         | $3.32 \times 10^{-3}/50$        | 30               |
| Capacitance ( $f/Km$ )     | $11.33 \times 10^{-9} \times 50$ | $5.01 \times 10^{-9} \times 50$ |                  |

The machines (M2, M3, M4) are set to supply (700 MW) meanwhile Machine (M1) and the WPP are set to supply (300 MW) and (400 MW) respectively. Therefore, the WPP partially shares the power

with Machine M1 to supply the grid together with (700 MW). This keeps the transferred power from Area 1 to Area 2 at (413 MW) as illustrated in the power flow analysis in Table 6.

Table 6. Power flow analysis of the system

| Bus        | Voltage          | P (MW)   | Q (MVAR) |
|------------|------------------|----------|----------|
| B1         | 0.99 pu   230kV  | -948.18  | 320.28   |
| B2         | 1.003 pu   230kV | -1776.08 | 479.09   |
| WPP        | 1 pu   0.575kV   | 400      | -43.81   |
| M1         | 1 pu   20kV      | 300      | -83.94   |
| M2 (Slack) | 1 pu   20kV      | 708.47   | -127.63  |
| M3         | 1 pu   20kV      | 719      | -82.57   |
| M4         | 1 pu   20kV      | 700      | -83.45   |

### 3. SYSTEM IDENTIFICATION

Each conventional machine in the system, as mentioned in Section 0, has a governor, AVR, and PSS. In this study, a new control technique is introduced to be a PSS and this requires getting the state-space model of the machine. So, a system identification method is used to get the model. In this method, only input-output data are needed to calculate the linearized model. The system is treated as a black box. A known signal is injected at the system input and the output signal is observed. Therefore, the MATLAB algorithm (N4SID) yields the state-space matrices. These matrices can be computed in continuous and discrete forms. N4SID [19] is a non-iterative algorithm that uses QR and singular value decompositions. It needs only the order of the system. Also, it can investigate the system's order through the dominant singular values of a matrix computed during the identification. The calculated state-space matrices can be generated in canonical forms.

The system has four conventional machines with the same ratings but three of them have the same operating points except that of the machine parallel to the WPP. As the PSS is a local controller implemented to the conventional machines, the model of each one should be calculated. Therefore, system identification is used to get a local state-space model for each of them.

The input and output signals are chosen to be the input signal of the PSS and the frequency change of the machine, respectively, as shown in Fig. 3. The input signal should have enough excitation to get an accurate model. The excitation depends on the input signal amplitude and frequency. It is selected to be a square wave with 0.02 pu and -0.02 pu maximum and minimum limits respectively. Its duty period is 20 seconds with a 50% pulse width. This signal is inserted for enough time to collect sufficient information about the system. The sampling period is chosen to be 0.005 seconds.

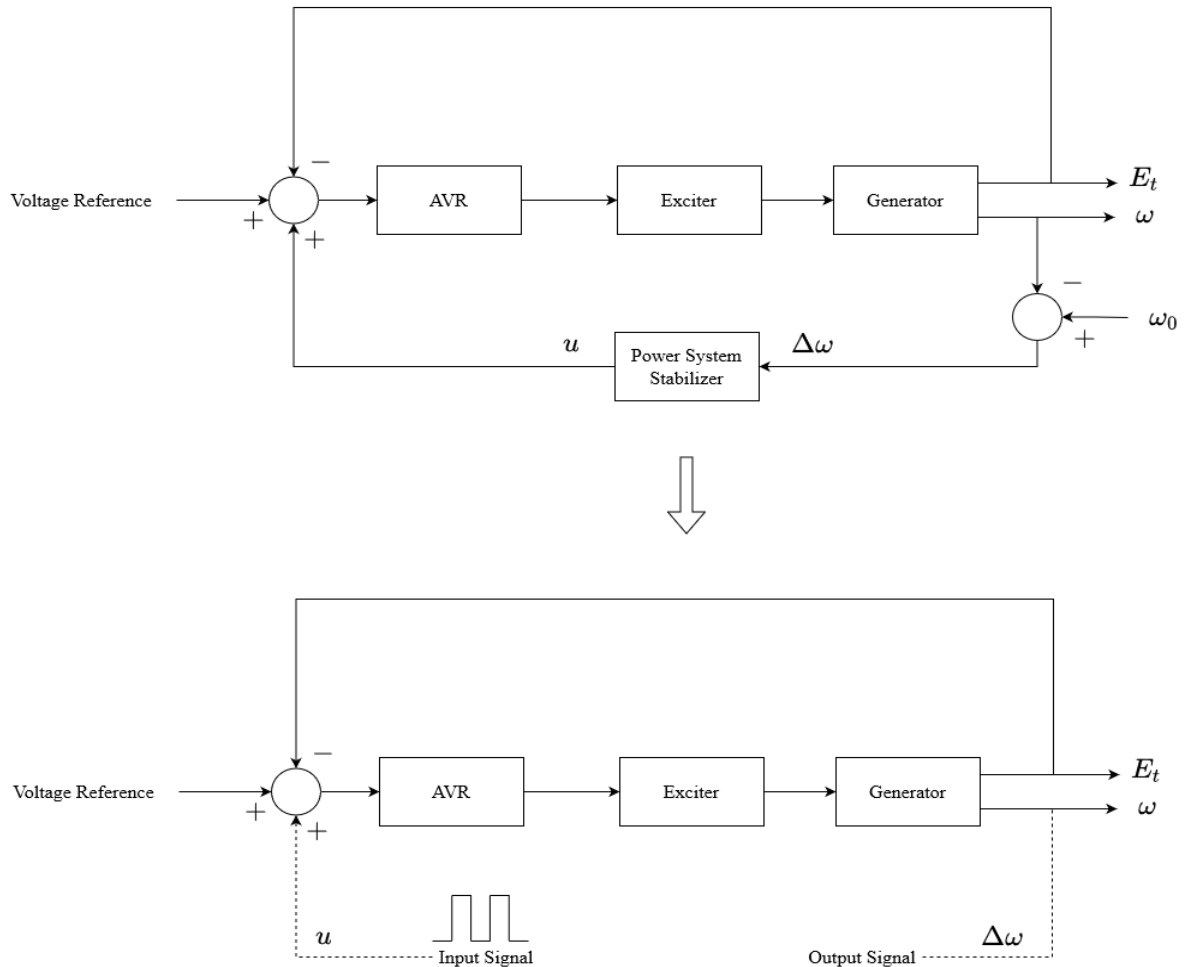


Figure 3. Machine preparation to system identification.

The input and output signals, Fig. 4, are processed by the MATLAB system identification toolbox [20]. The predicted system's order is chosen to be 4 to correspond to the typical dominant dynamics. The used identification algorithm is determined (N4SID). The state-space form is determined as the observable canonical form. These steps are repeated to get the model of the four machines.

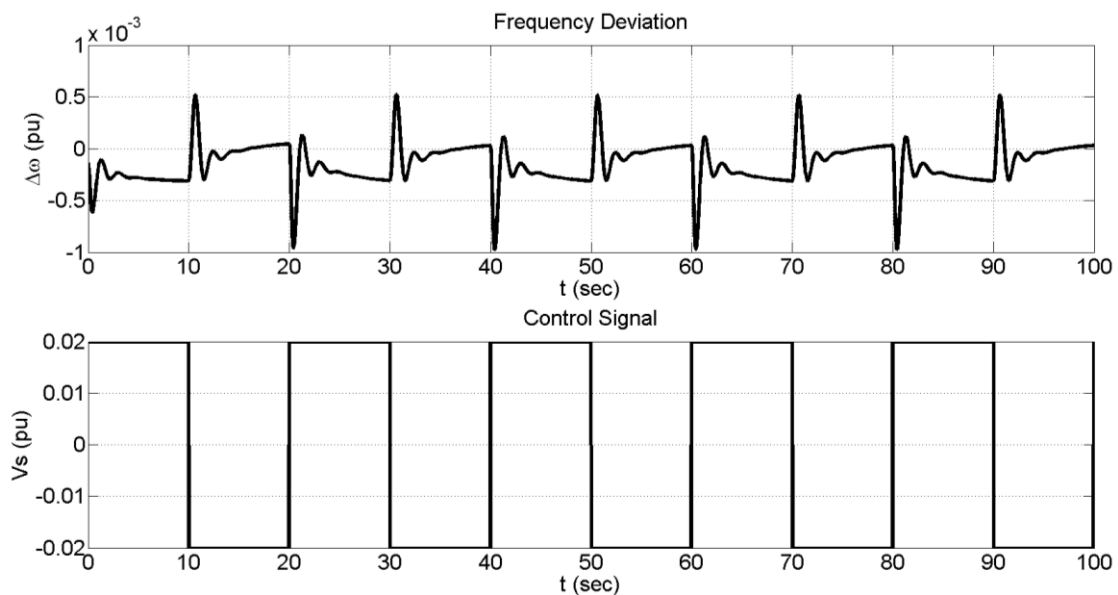


Figure 4. Input-output signals in system identifications.

The input and output are; the input signal of the PSS ( $u$ ) and the frequency change ( $\Delta\omega$ ) respectively. The first state is defined as the output ( $\Delta\omega$ ) and the others are defined as a mathematical combination of the input and the output. Then, the discrete state-space matrices, continuous transfer function, and poles of Machine (M1) are obtained in Eqs. 1, 2, 3, respectively.

$$A_{M1} = \begin{bmatrix} 0 & 1 & 0 & 0 \\ 0 & 0 & 1 & 0 \\ 0 & 0 & 0 & 1 \\ 0.9263 & -1.837 & -0.1029 & 2.0136 \end{bmatrix} \quad (1)$$

$$B_{M1} = 10^{-4} \begin{bmatrix} -0.0241 \\ -0.1586 \\ -0.2836 \\ -0.4101 \end{bmatrix}$$

$$C_{M1} = [1 \quad 0 \quad 0 \quad 0]$$

$$tf_{M1} = \frac{-9357s - 3378}{s^4 + 17450s^3 + 107200s^2 + 723500s + 626400} \quad (2)$$

$$P_{M1} = \{-17442, \quad -3 + 5j, \quad -3 - 5j, \quad -1\} \quad (3)$$

The data shows that there are; a pole near to the imaginary axis on the left side of the real axis, two complex poles near to the imaginary axis, and a pole so far on the left side of the real axis. The complex poles are dominant and make the system's response oscillatory, meanwhile, the far pole effect vanishes quickly, and the near pole is slow.

The data of the other machines are included in Appendix A. All machines have two complex poles near the imaginary axis and two real poles on the left side of the real axis. One of the real poles is far away from the other poles on the left side of the real axis. So, it has a small effect on the response as it vanishes quickly.

#### 4. MODEL PREDICTIVE CONTROL

Model predictive control (MPC) uses mathematical optimization techniques to get the optimal control output as shown in Ref. [21]. It can handle large-scale systems and consider the input and states constraints. Consequently, it achieves a high degree of stability and robustness. For these merits, it is proposed to be used as a PSS because the PSS has constraints on the control signal as will be shown in Section 0.

Its strategy starts with getting the state-space matrices of the system. Then, the states and control output are easily predicted. The prediction may be for a finite or infinite horizon. Then, a numerical optimization technique is used to get the optimal control action. The optimization algorithm considers the input and state constraints. After getting the state-space matrices Eq. 4 by system identification, the predicted states vector can be computed in Eq. 5 as follows:

$$\begin{aligned} x(k+1) &= Ax(k) + Bu(k) \\ y(k) &= Cu(k) \end{aligned} \quad (4)$$

Here,  $x(k)$  and  $u(k)$  are the states and input vectors at instant  $k$ , respectively.  $A$ ,  $B$ , and  $C$  are the system matrices in this respect.

$$\begin{bmatrix} x(k+1|k) \\ x(k+2|k) \\ x(k+3|k) \\ \vdots \\ x(k+N|k) \end{bmatrix} = \begin{bmatrix} A \\ A^2 \\ A^3 \\ \vdots \\ A^N \end{bmatrix} x(k) + \begin{bmatrix} B & 0 & 0 & \dots & 0 \\ AB & B & 0 & \dots & 0 \\ A^2B & AB & B & \dots & 0 \\ \vdots & \vdots & \vdots & \vdots & \vdots \\ A^{N-1}B & A^{N-2}B & \dots & \dots & B \end{bmatrix} \begin{bmatrix} u(k|k) \\ u(k+1|k) \\ u(k+2|k) \\ \vdots \\ u(k+N-1|k) \end{bmatrix}$$

$$X(k) = Mx(k) + cU(k) \tag{5}$$

Here,  $N$  is the prediction horizon.  $x(k|k)$  &  $u(k|k)$  are the states and input vectors at  $k$ .  $x(k+i|k)$  and  $u(k+i|k)$  are the predicted states and input vectors at  $k+i$  based on information available at  $k$ .  $X(k)$  and  $U(k)$  are the total predicted states and total input vectors based on information available at  $k$ . Then, the objective function, Eq. 6, which consists of the predicted states and control outputs, is minimized to get the optimal control action  $u(k)$ .

$$J(k) = \sum_{i=0}^{N-1} [x^T(k+i|k)Qx(k+i|k) + u^T(k+i|k)Ru(k+i|k)] + x^T(k+N|k)\bar{Q}x(k+N|k) \tag{6}$$

Here,  $Q$  and  $R$  are the weighting matrices.  $\bar{Q}$  is the terminal weighting matrix which is calculated by solving the Lyapunov equation Eq. 7:

$$\bar{Q} - (A+BK)^T\bar{Q}(A+BK) = Q + K^TRK \tag{7}$$

Here,  $K$  is feedback gain. By combining Eqs. 8 and 9, the objective function becomes as in Eq. 10:

$$J(k) = U(k)^T H U(k) + 2x^T(k)F^T U(k) + x^T(k)Gx(k) \tag{8}$$

Here,

$$\begin{aligned} H &= c^T \bar{Q} c + \bar{R} \\ F &= c^T \bar{Q} M \end{aligned} \tag{9}$$

$$G = M^T \bar{Q} M + Q$$

$$\bar{Q} = \begin{bmatrix} Q & 0 & \dots & 0 \\ 0 & Q & \dots & 0 \\ 0 & \dots & \ddots & 0 \\ 0 & 0 & \dots & \bar{Q} \end{bmatrix} \tag{10}$$

$$\bar{R} = \begin{bmatrix} R & 0 & \dots & 0 \\ 0 & R & \dots & 0 \\ 0 & \dots & \ddots & 0 \\ 0 & 0 & \dots & R \end{bmatrix}$$

exist. The system has constraints in the control input which should be considered in the optimization process so they are written as in Eqs. 11, 12.

$$\begin{bmatrix} u_{min} \\ u_{min} \\ \vdots \\ u_{min} \end{bmatrix}_{N*1} \leq \begin{bmatrix} u(k|k) \\ u(k+1|k) \\ \vdots \\ u(k+N-1|k) \end{bmatrix}_{N*1} \leq \begin{bmatrix} u_{max} \\ u_{max} \\ \vdots \\ u_{max} \end{bmatrix}_{N*1} \tag{11}$$

$$[u_{min}]_{N*1} \leq [I_N]U(k) \leq [u_{max}]_{N*1}$$

$$\begin{aligned} \begin{bmatrix} I_N \\ -I_N \end{bmatrix}_{2N \times N} U(k) &\leq \begin{bmatrix} u_{max} \\ -u_{min} \end{bmatrix}_{2N \times 1} \\ A_c U(k) &\leq b_0 \end{aligned} \quad (12)$$

By considering these constraints, the controller becomes nonlinear and the closed-loop system becomes nonlinear consequently. So the linear stability studying methods can't be used. Lyapunov stability laws should be used instead which require three conditions to ensure the system's stability. According to Lyapunov, our case achieves two stability conditions; the weighting matrix  $Q$  is positive definite and the terminal weighting matrix  $\bar{Q}$  ensures infinite perdition horizon. The last one is that the predicted control outputs at the next steps should satisfy the constraints as well. The predicted control outputs at the next steps are called the tail of the control output at  $(k)$  presented in Fig. 5. Hence, additional constraints are required to achieve the third condition. They are written in Eq. 13.

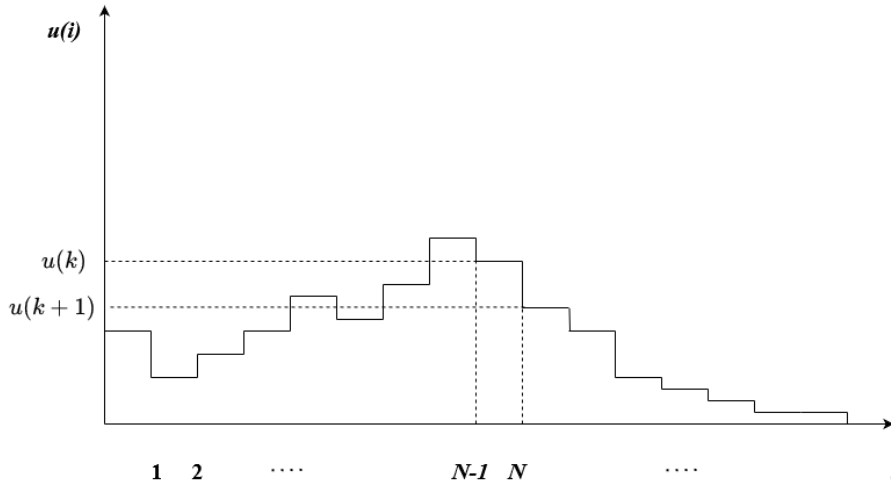


Figure 5. The predicted control output and its tail graph.

$$u_{min} \leq u(k + i|k) \leq u_{max} \quad (13)$$

Here,

$$i = 0, 1, 2, \dots, \infty$$

stands. Instead of checking this constraint for infinite steps, it is enough to check it for enough finite number of steps which is called the minimum control horizon ( $N_c$ ). After these steps, the control action is decreasing so it keeps the constraints consequently. To investigate this number ( $N_c$ ) and its additional constraints, the general equation of the tail is calculated from the state space matrices as in Eq. 14.

$$u(k + i|k) = K(A + BK)^i x(k) \quad (14)$$

where,

$$i = 0, 1, 2, \dots, N_c$$

So the additional constraints in Eq. 14 can be written as in Eq. 15.

$$u_{min} \leq K(A + BK)^i x(k) \leq u_{max} \quad (15)$$

The additional constraints are linear and can be solved by a linear programming algorithm. The flowchart of the used algorithm is illustrated in Fig. 6. The algorithm gives the tail matrix ( $A_{tail}$ ) and the minimum control horizon ( $N_c$ ). Therefore, the tail equation is Eq. 16.

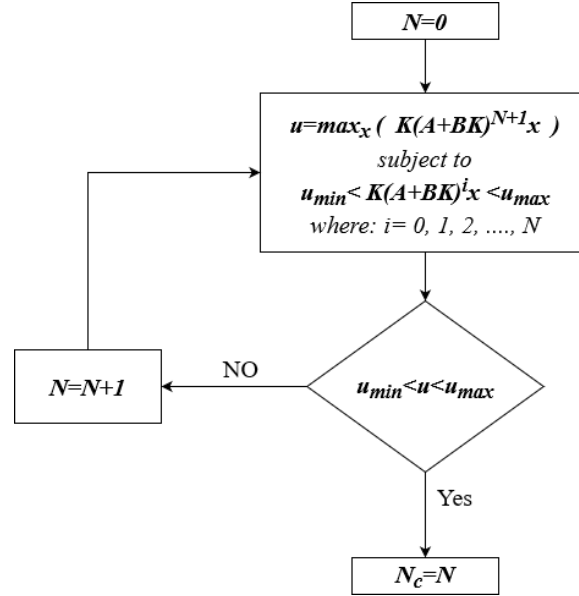


Figure 6. Additional stability constraints algorithm flowchart

$$U(k+1) = A_{tail}x(k)$$

$$A_{tail} = \begin{bmatrix} K \\ K(A+BK) \\ \vdots \\ K(A+BK)^{N_c} \end{bmatrix}_{(N_c+1)*N} \quad (16)$$

The predicted control actions satisfy the tail constraints until  $(N - 1)$ . That's why it is already considered with the inputs and states constraints. So the tail of the final predicted term at  $(N)$  only needs to satisfy the constraints. From Eqs. 16, 17, the tail equation of the final predicted term at  $(N)$  is Eq. 18.

$$U(k+N+1) = A_{tail}\{A^N x(k) + [A^{N-1}B \quad A^{N-2}B \quad \dots \quad B]U(k)\} = A_1 x(k) + A_2 U(k) \quad (17)$$

$$A_1 = A_{tail}A^N$$

$$A_2 = A_{tail}[A^{N-1}B \quad A^{N-2}B \quad \dots \quad B]$$

So the additional constraints Eq. 17 can be written as Eq. 18.

$$\begin{bmatrix} u_{min} \\ \vdots \\ u_{min} \end{bmatrix}_{(N_c+1)*1} \leq A_1 x(k) + A_2 U(k) \leq \begin{bmatrix} u_{max} \\ \vdots \\ u_{max} \end{bmatrix}_{(N_c+1)*1} \quad (18)$$

Then, it can be reduced to Eq. 19.

$$\begin{bmatrix} A_2 \\ -A_2 \end{bmatrix}_{2(N_c+1)*N} U(k) \leq \begin{bmatrix} u_{max} \\ -u_{min} \end{bmatrix}_{2(N_c+1)*1} + \begin{bmatrix} -A_1 \\ A_1 \end{bmatrix}_{2(N_c+1)*N} x(k) \quad (19)$$

Therefore, the total constraints can be collected from Eqs. 19, and written as Eq. 20.

$$\begin{bmatrix} I_N \\ -I_N \\ A_2 \\ -A_2 \end{bmatrix}_{2(N+N_c+1)*N} U(k) \leq \begin{bmatrix} u_{max} \\ -u_{min} \\ u_{max} \\ -u_{min} \end{bmatrix}_{2(N+N_c+1)*1} + \begin{bmatrix} 0_N \\ 0_N \\ -A_1 \\ A_1 \end{bmatrix}_{2(N+N_c+1)*N} x(k) \quad (20)$$

$$A_{cons}U(k) \leq B_{cons} + C_{cons}x(k)$$

Thus, the objective function Eq. 19 can be optimized by considering the constraints Eq. 20 to get the optimal control output by using quadratic programming techniques like active-set or interior-point methods. The control output is computed repeatedly at each step by solving a quadratic optimization problem using the MATLAB command as in Eq. 21.

$$u(k) = \text{quadprog}(H, Fx(k), A_{cons}, B_{cons} + C_{cons}x(k)) \quad (21)$$

### 5. POWER SYSTEM STABILIZER

The PSS is a local controller installed in conventional machines to damp the frequency oscillations via the excitation system as shown in Fig. 7. To keep the excitation system working properly, the PSS has limits on its control output in the range of  $(\pm 0.1 pu)$ . A state observer is needed due to the unmeasurable states of the system as mentioned in Section 0.

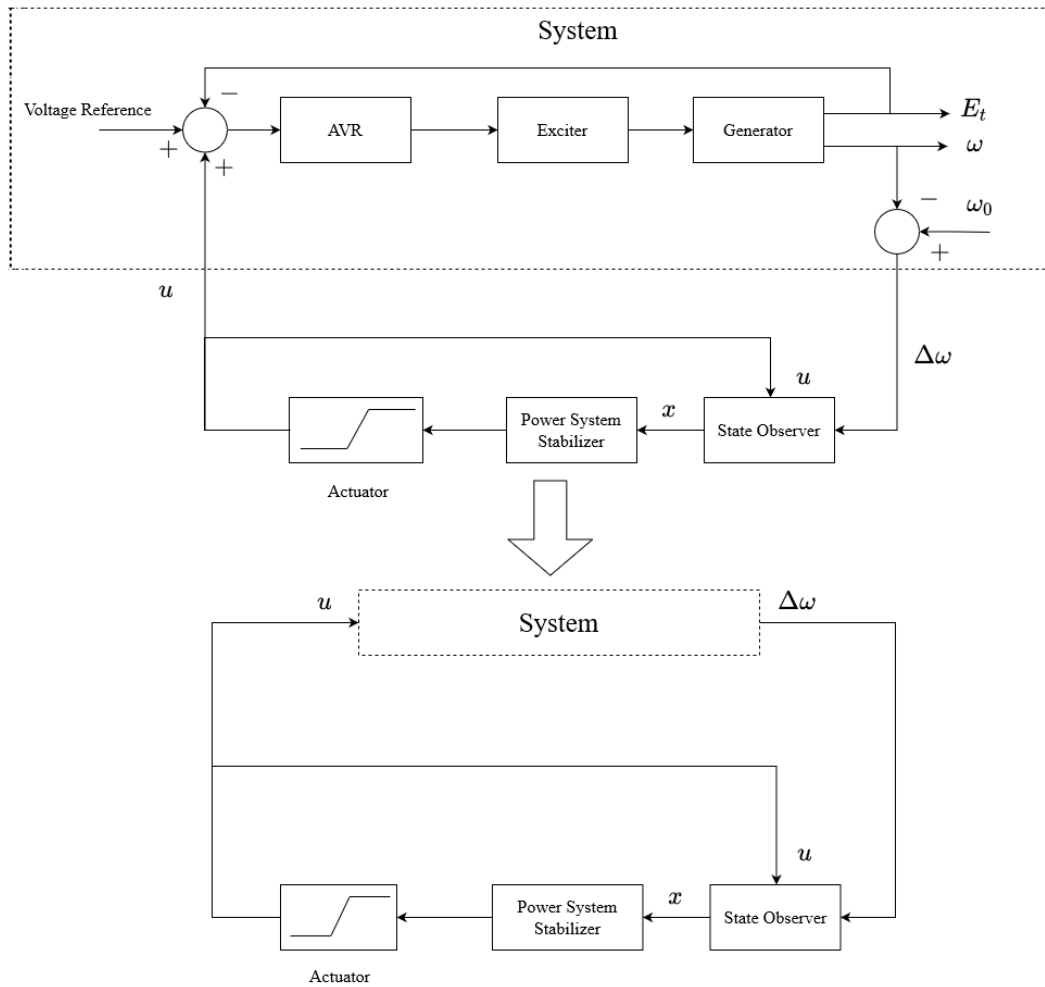


Figure 7. Closed-loop system block diagram.

In this paper, two other controllers are implemented and compared to the MPC; conventional multi-band control (MB) and linear quadratic regulator (LQR). The controllers are designed and applied to the four conventional machines. Then, the performance of the controllers is investigated and compared to each other.

Before starting in MPC design, a state observer is firstly considered to estimate the states which are used in the controller. A full state observer is designed because most of the states are mathematical and cannot be measured practically.

### 5.1. State Observer

The observability matrices of the machines have full rank, so their systems are completely observable. The desired observer poles are chosen to be faster than that of the systems. Then, they are computed in the discrete form as in [22]. Hence, the desired observer poles of Machine (M1) are given in Eq. 22. Its observer gain is calculated via Ackerman's formula. The result is given by Eq. 23. Similarly, the results for the other machines are computed and included in *Appendix A*.

$$P_{o_{M1}} = \{0, 0.9494 + 0.0259j, 0.9494 - 0.0259j, 0.9805\} \quad (22)$$

$$K_{o_{M1}} = [-0.8656, 0.9177, -0.7844, 0.8426] \quad (23)$$

The design is performed as shown in Section 2. The weighted matrices are chosen as in Eq. 24 so the weighting matrices become equal for all of the machines. Then, the prediction horizon is chosen to be ( $N = 10$ ).

$$Q = 100 I_{4 \times 4} = \begin{bmatrix} 100 & 0 & 0 & 0 \\ 0 & 100 & 0 & 0 \\ 0 & 0 & 100 & 0 \\ 0 & 0 & 0 & 100 \end{bmatrix} \quad (24)$$

$$R = 0.0001$$

So the minimum control horizon for Machine (M1) is in Eq. 25. Hence, the control inputs are calculated repeatedly at each sample as in Eq. 24. The results for the other machines are computed and included in *Appendix A*.

$$N_{c_{M1}} = 32 \quad (25)$$

### 5.2. Linear Quadratic Regulator

The state observers designed in Section 0 will provide state information for the LQR. In addition, the weighting matrices are chosen typically like MPC as in Eq. 24. Therefore, the LQR gain for Machine (M1) is calculated as in Ref. [22] in Eq. 26. Similarly, gains of the other machines are computed and included in *Appendix A*.

$$K_{LQR_{M1}} = [-23810 \quad 28858 \quad 25446 \quad -32296] \quad (26)$$

### 5.3. Multi-Band Controller

The used MB PSS is implemented with the simplified parameters (PSS4B) according to IEEE standards 421.5 [17]. Its parameters are listed in Table 7.

Table 7. MB PSS parameters

| Global Gain                 | 1   |
|-----------------------------|---|
| Low Frequency Band          | $F_L = 0.2 \text{ Hz}, \quad K_L = 30$                            |
| Intermediate Frequency Band | $F_I = 1.25 \text{ Hz}, \quad K_I = 40$                           |
| High Frequency Band         | $F_H = 12 \text{ Hz}, \quad K_H = 160$                            |
| Signals Limits              | $V_{L_{\max}} = V_{I_{\max}} = V_{H_{\max}} = V_{S_{\max}} = 0.1$ |

## 6. RESULTS AND DISCUSSION

After applying the proposed PSSs to the machines, the system reaches a steady state. To analyze and study the performance of the PSSs, three common tests are nominated; three-phase fault, transmission line outage, and voltage reference of a machine sudden change. This study monitors the settling time ( $T_s$ ) and the peak value ( $P.V.$ ) of the machines' frequency deviation and the tie-line power oscillations in each test.

### 6.1. Three-Phase Fault

While the system operates normally, a three-phase fault suddenly happens in the middle of one of the inter-area transmission lines. This fault lasts for 200 ms before the protection devices clear it. All controllers damp the tie-line power and frequency oscillations well as shown in Figs. 8 and 9, respectively.

The constrained MPC and LQR outperform the MB controller. They give the shortest settling time nearly (7.6 sec) in the tie-line power. The MB comes lastly in the third position with around (13 sec), see Fig. 8. In addition, their response gets approximately the same peak value (0.69 pu) which is slightly high because the PSS controls directly the frequency deviation and therefore it affects and controls the tie-line power indirectly.

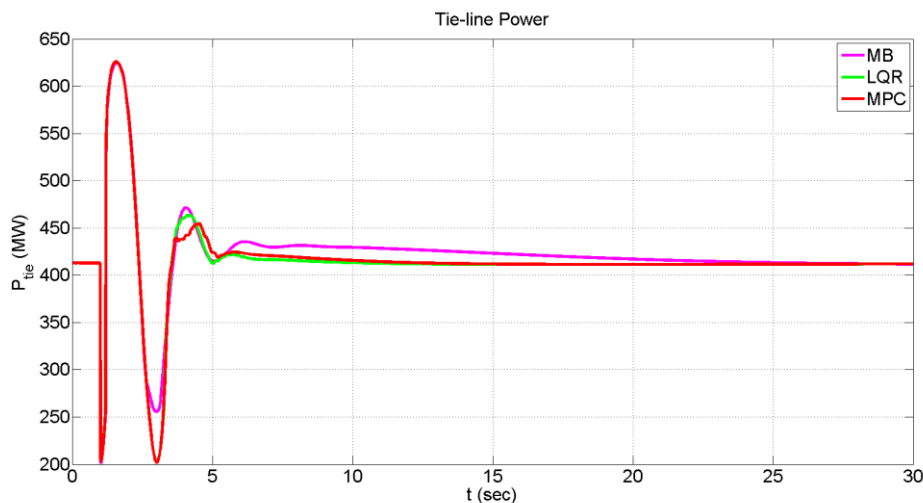


Figure 8. Time response of the tie-line power in the three-phase fault test.

Focusing on the frequency deviation of the machines, MPC and LQR damp the oscillations faster than MB, Fig. 9. However, the frequency deviation is small for all controllers. There is no need to exceed the constraints of the actuator, so the results of the MPC and LQR are slightly the same.

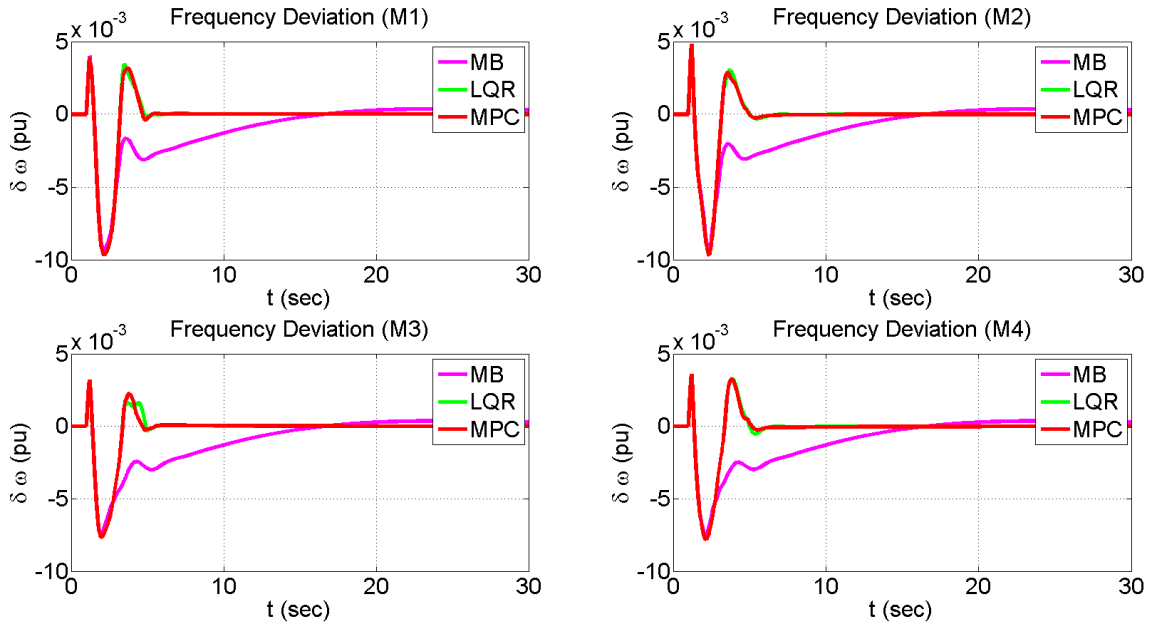


Figure 9. Time response of frequency deviation in three-phase fault test.

Also, the relative frequencies of the machines are so small in most of the cases but their values with MPC are smaller than that with LQR in some cases like between M3 and M4, Fig. 10.

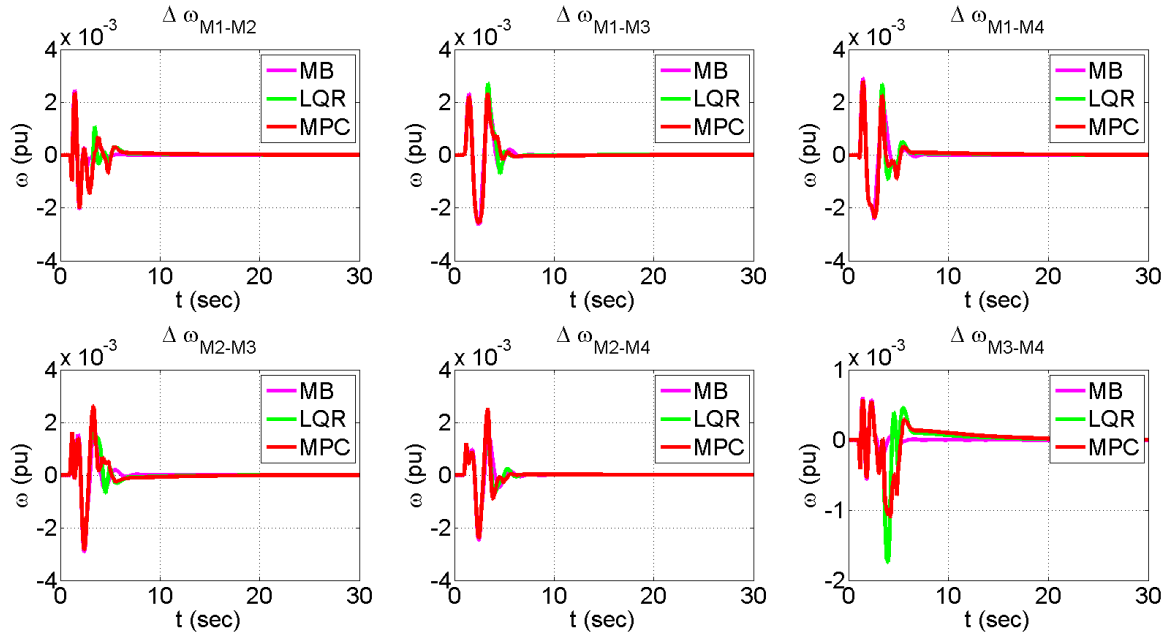


Figure 10. Relative frequency deviation in three-phase fault test.

## 6.2. Transmission Line Outage

While the system operates normally, one of the inter-area transmission lines is suddenly cut for 135 ms and then it is back. The system still operates without that transmission line during this period. All controllers damp the tie-line power and frequency oscillations as exposed in Figs. 11 and 12, respectively.

The constrained MPC and LQR outperform the MB controller. MPC performs slightly faster than LQR and gives the shortest settling time nearly (3.53 sec) in the tie-line power meanwhile LQR comes secondly with (4.3 sec) and MB in the third position, Fig. 11. Accordingly, that proves the efficiency of MPC in handling the input constraints. In addition, their response gets approximately the same peak value (0.6 pu).

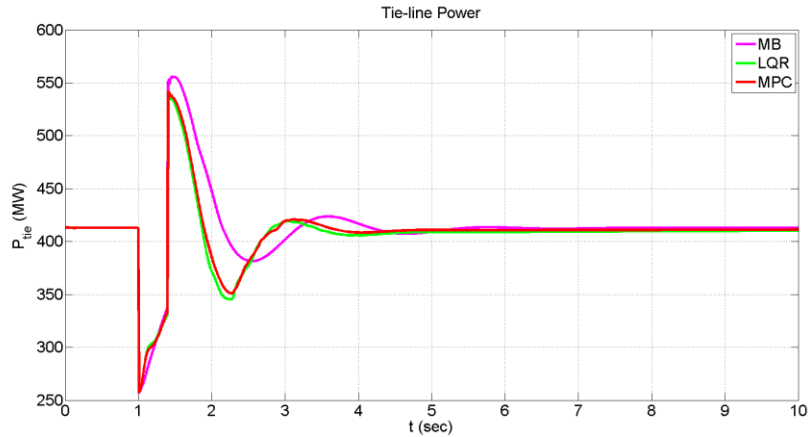


Figure 11. Time response of the tie-line power in the transmission line outage test.

For the frequency deviation of the machines, MPC and LQR damp the oscillations faster than MB as well, but MPC is slightly faster in some machines, Fig. 12. Still, the frequency deviation is small with all of the controllers.

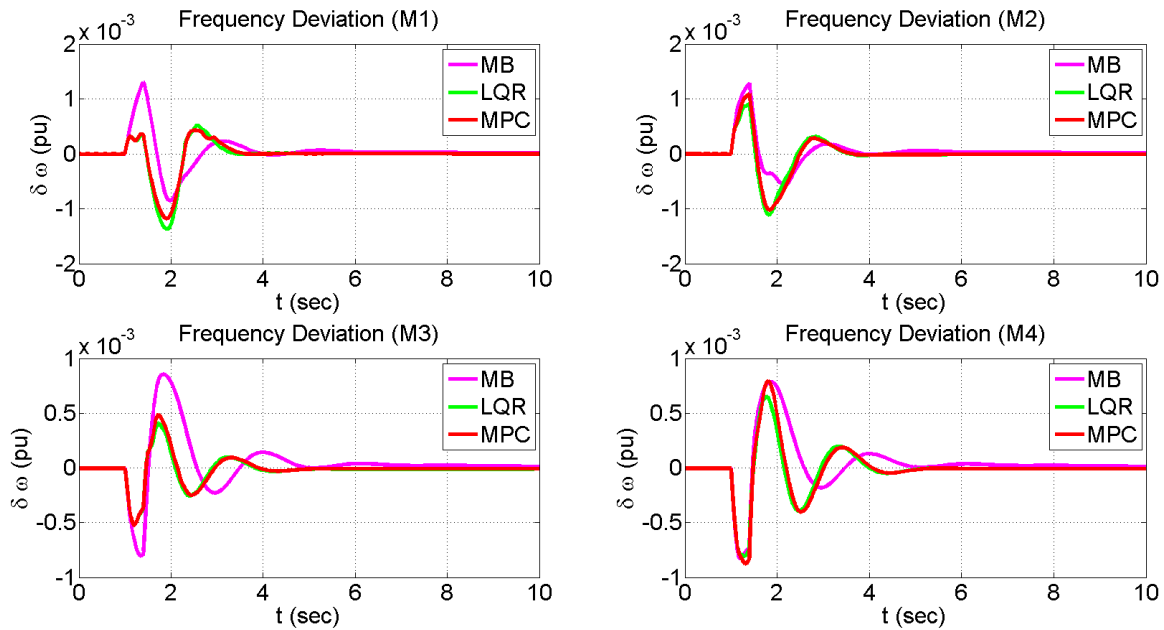


Figure 12. Time response of frequency deviation in the transmission line outage test.

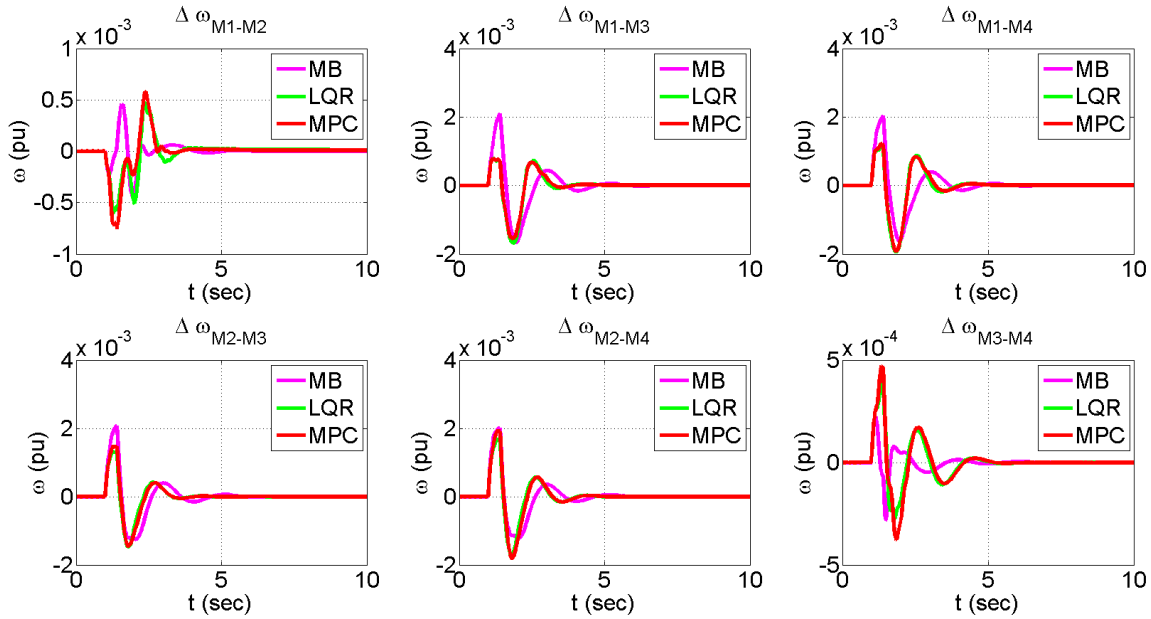


Figure 13. Relative frequency deviation of the machines in the transmission line outage test

Moreover, the relative frequencies of the machines are shown in Fig. 13. MPC and LQR exhibit smaller oscillations compared to that with the MB in some cases like the relative oscillations between M1 and M3.

### 6.3. Voltage Reference Sudden Change

During the normal operation of the power system, the voltage reference of Machine (M1) is suddenly changed from 1 pu to 1.05 pu and then back to 1 pu after 200 milliseconds. All of the controllers damp the tie-line power and frequency oscillations well as presented in Figs. 14 and 15 in turn.

The constrained MPC gives the shortest settling time (3.29 sec) to retrieve the tie-line power. Meanwhile, the LQR comes in the second position with (3.47 sec) and the MB is in the last position, Fig. 14. In addition, their response gets approximately the same peak value (0.47 pu). So, that demonstrates the productivity of MPC in handling the constraints.

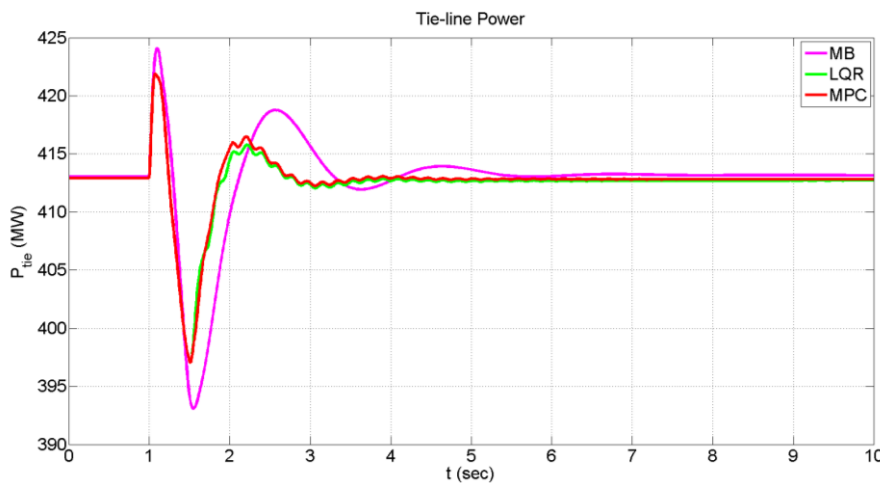


Figure 14. Time response of the tie-line power in the voltage reference sudden change test

In the frequency deviation of the machines, MPC and LQR damp the oscillations faster than MB as well but MPC is slightly faster in some machines (Fig. 15).

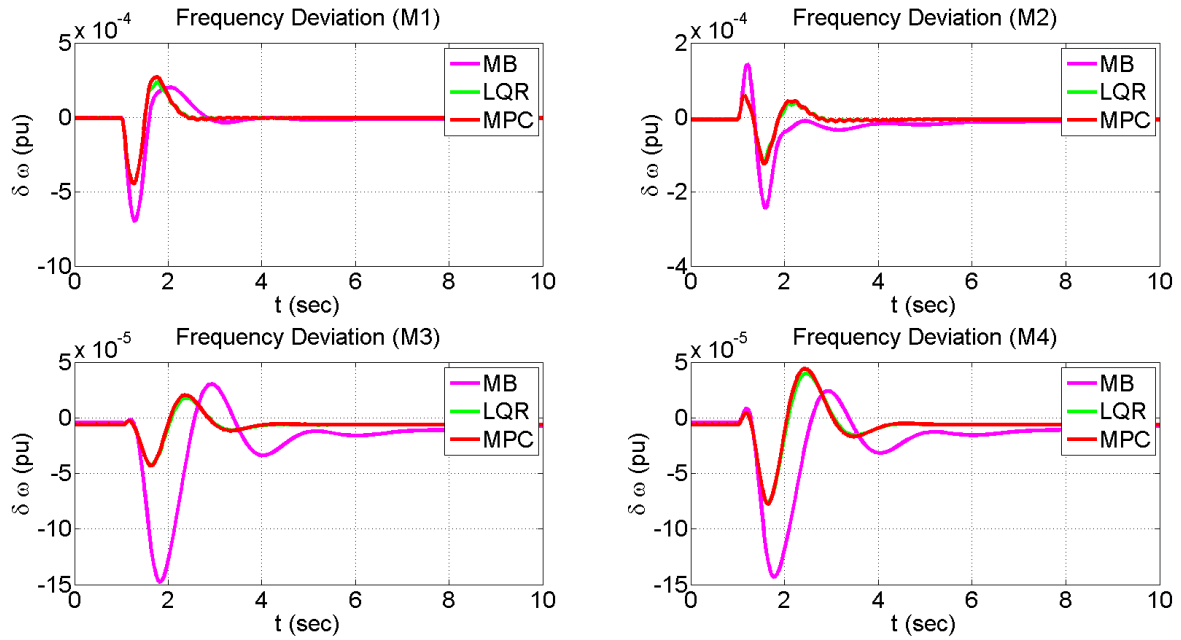


Figure 15. Time response of frequency deviation in the voltage reference sudden change test.

The relative frequencies of the machines using MPC and LQR controllers are smaller than that with MB in some cases as well (Fig. 16).

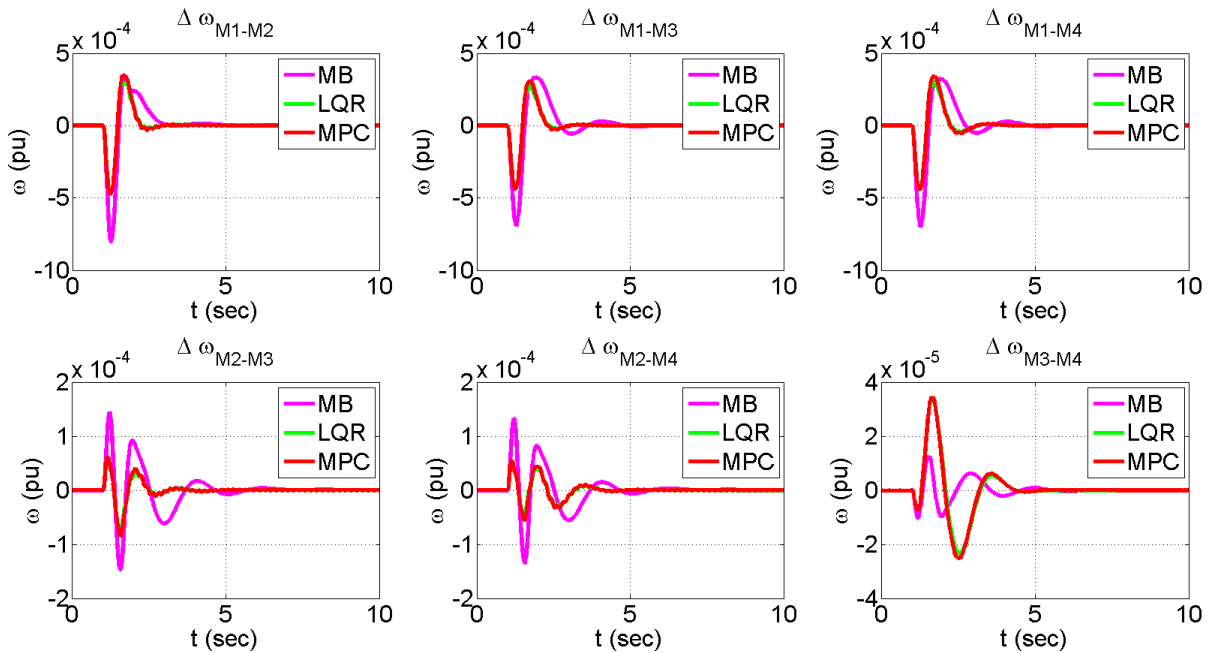


Figure 16. Relative frequency deviation in the voltage reference sudden change test.

The characteristics of the time response of the controllers in each test are summarized in Table 8. They include the settling time ( $T_s$ ) in seconds, the peak value ( $P.V.$ ) in per-unit and the damping ratio ( $\zeta$ ). The system with all of the controllers is underdamped because the damping ratio is in the range of  $(0 < \zeta < 1)$  [22]. The overall results indicate that the conventional MB PSS may need to be replaced by the proposed controller.

*Table 8. Comparison of the closed-loop response of the PSSs.*

| Controller Type                            | Three-Phase Fault |        |         | Transmission Line Outage |        |         | Voltage Reference Sudden Change |         |         |
|--|-------------------|--------|---------|--------------------------|--------|---------|---------------------------------|---------|---------|
|  | $T_s$             | $P.V.$ | $\zeta$ | $T_s$                    | $P.V.$ | $\zeta$ | $T_s$                           | $P.V.$  | $\zeta$ |
| <i>Frequency Deviation of Machine (M1)</i> |                   |        |         |                          |        |         |                                 |         |         |
| MB   | 17.4              | 0.0095 | 0.99    | 5.8                      | 0.0012 | 0.99    | 3.6                             | 0.0008  | 0.99    |
| LQR  | 5.02              | 0.0097 | 0.99    | 3.25                     | 0.0014 | 0.99    | 2.8                             | 0.0004  | 0.99    |
| MPC  | 5.1               | 0.0097 | 0.99    | 3.47                     | 0.0012 | 0.99    | 2.8                             | 0.0004  | 0.99    |
| <i>Frequency Deviation of Machine (M2)</i> |                   |        |         |                          |        |         |                                 |         |         |
| MB   | 17.4              | 0.0094 | 0.99    | 5.68                     | 0.0011 | 0.99    | 6.16                            | 0.0004  | 0.99    |
| LQR  | 6                 | 0.0097 | 0.99    | 3.5                      | 0.0011 | 0.99    | 4.2                             | 0.0001  | 0.99    |
| MPC  | 5.68              | 0.0097 | 0.99    | 3.5                      | 0.0011 | 0.99    | 4.2                             | 0.0001  | 0.99    |
| <i>Frequency Deviation of Machine (M3)</i> |                   |        |         |                          |        |         |                                 |         |         |
| MB   | 17.8              | 0.0076 | 0.99    | 6.6                      | 0.0009 | 0.99    | 8.34                            | 0.0003  | 0.99    |
| LQR  | 5.26              | 0.0077 | 0.99    | 4.7                      | 0.0005 | 0.99    | 3.97                            | 0.00004 | 0.99    |
| MPC  | 5.19              | 0.0077 | 0.99    | 4.7                      | 0.0005 | 0.99    | 3.96                            | 0.00004 | 0.99    |
| <i>Frequency Deviation of Machine (M4)</i> |                   |        |         |                          |        |         |                                 |         |         |
| MB   | 17.8              | 0.0076 | 0.99    | 6.6                      | 0.0009 | 0.99    | 8.4                             | 0.0003  | 0.99    |
| LQR  | 5.98              | 0.0078 | 0.99    | 4.8                      | 0.0008 | 0.99    | 4.1                             | 0.00007 | 0.99    |
| MPC  | 5.9               | 0.0078 | 0.99    | 4.8                      | 0.0008 | 0.99    | 4.1                             | 0.00007 | 0.99    |
| <i>Tie-Line Power</i>                      |                   |        |         |                          |        |         |                                 |         |         |
| MB   | 21.1              | 0.69   | 0.2     | 5.06                     | 0.62   | 0.31    | 5.07                            | 0.47    | 0.8     |
| LQR  | 7.56              | 0.69   | 0.2     | 4.3                      | 0.59   | 0.34    | 3.47                            | 0.47    | 0.8     |
| MPC  | 7.66              | 0.69   | 0.2     | 3.53                     | 0.6    | 0.34    | 3.29                            | 0.47    | 0.8     |

## 7. CONCLUSIONS

This paper proposes a PSS design based on constrained MPC. The objective is to damp the inter-area oscillations of a multi-machine power system that includes a wind power plant. For comparison purposes, the conventional MB-PSS and LQR are implemented. All PSSs are tested against disturbances, three-phase fault, a transmission line outage, and a sudden change of a generator's reference voltage.

The study has shown that all the controllers have succeeded in damping the frequency and tie-line oscillations in the presence of the WPP in the case of partial power-sharing. The PSS design based on constrained MPC has handled the input constraints efficiently, and this has been evident in the used tests. LQR performs well in damping the frequency oscillations and generally acts similar to MPC in the absence of constraints. Although the conventional MB damps the frequency and tie-line power oscillation, the other controllers are faster. This indicates that MPC-PSS and LQR-PSS outperform the conventional MB-PSS may need to be re-tuned with the integration of the WPP to the grid.

To conclude, PSSs can still succeed in damping the oscillations that follow disturbances in power systems that have wind penetrations. Constrained MPC can handle the input constraints and effectively damp the oscillations.

## REFERENCES

- [1] Renewable Capacity Statistics 2020. International Renewable Energy Agency (IRENA), 2020.
- [2] IEEE Recommended Practice for Excitation System Models for Power System Stability Studies. IEEE Std 421.5-2005 (Revision of IEEE Std 421.5-1992) 2006; 10 Aug. 1992: IEEE, pp. 1-93.
- [3] IEEE Recommended Practice for Excitation System Models for Power System Stability Studies. IEEE Std 421.5-2016 (Revision of IEEE Std 421.5-2005) 2016; 15 May 2016: IEEE: pp. 1-207.

- [4] Chen, S, Malik, OP, Chen, T. A Robust Power System Stabilizer Design. *Optimal Control Applications and Methods* 1997; 18(3): 179-193. DOI:10.1002/(SICI)1099-1514(199705/06)18:3<179::AID-OCA597>3.0.CO;2-5
- [5] Abdelazim, T, Malik, OP. Power System Stabilizer Based on Model Reference Adaptive Fuzzy Control. *Electrical Power Components and Systems* 2005; 33(9): 985-998. DOI:10.1080/15325000590921017
- [6] Harmas, N, Essounbouli, H. A New Robust Adaptive Fuzzy Sliding Mode Power System Stabilizer. *Electrical Power and Energy Systems* 2012; 42: 1-7. DOI:10.1016/j.ijepes.2012.03.032
- [7] Yee, SK, Milanović, JV. Fuzzy logic controller for decentralized stabilization of multimachine power systems. *IEEE Transactions on Fuzzy Systems* 2008; 16(4): 971-981. DOI:10.1109/TFUZZ.2008.917296
- [8] Changaroon, B., Srivastava, SC, Thukaram, D. A neural network-based power system stabilizer suitable for an online training-a practical case study for EGAT system. *IEEE Transactions on Energy Conversion* 2000; 15(1): 103-109. DOI:10.1109/60.849124
- [9] Chaturvedi, DK, Malik OP. Neuro-fuzzy Power System Stabilizer. *IEEE Transactions on Energy Conversion* 2008; 23(3): 887-894. DOI:10.1109/TEC.2008.918633
- [10] Soliman, M, Elshafei, AL, Bendary, F, Mansour, and W. Robust Decentralized PID-based Power System Stabilizer Design Using an ILMI Approach. *Electric Power System Research* 2010; 80(12): 1488-1497. DOI:10.1016/j.eprsr.2010.06.008
- [11] Ibrahim, H, Ghandour, M, Dimitrova, M, Ilinca, A, Perron, J. Integration of Wind Energy into Electricity Systems. Technical Challenges and Actual Solutions. *Energy Procedia* 2011; 6: 815-824. DOI:10.1016/j.egypro.2011.05.092
- [12] Kalogiannis, T, Llano, EM, Hoseinzadeh, B, da Silva, FF. Impact of high level penetration of wind turbines on power system transient stability: *IEEE Eindhoven PowerTech* 2015; 7232312: 1-6. DOI:10.1109/PTC.2015.7232312
- [13] Yang, J, Sun, X, Liao, K, He, Z, Cai, L. Model predictive control-based load frequency control for power systems with wind-turbine generators. *IET Renewable Power Generation* 2019; 13(15): 2871–2879. DOI: 10.1049/iet-rpg.2018.6179
- [14] Dang, DQ, Wu, S, Wang, Y, Cai, W. Model Predictive Control for maximum power capture of variable speed wind turbines. In: *IPEC 2010 International Power Engineering Conference*; 27-29 Oct. 2010: IEEE, pp.274-279. DOI:10.1109/IPEC.2010.5697119
- [15] Zhao, H, Wu, Q, Guo, Q, Sun, H, Huang, S, Xue, Y. Coordinated Voltage Control of a Wind Farm Based on Model Predictive Control. *IEEE Transactions on Sustainable Energy* 2016; 7(4): 1440-1451. DOI:10.1109/TSTE.2016.2555398
- [16] Kundur, P. *Power System Stability, and Control*. New York, USA: McGraw-Hill, Inc, 1994.
- [17] Klein, M, Rogers, GJ, Moorty, S, Kundur, P. Analytical investigation of factors influencing power system stabilizers performance. *IEEE Transactions on Energy Conversion* 1992; 7(3): 382-390. DOI: 10.1109/60.148556.
- [18] Ashraf, M, Elshafei, AL, Eldeeb, A. *Wind Power Plant Modeling and Control Design for Inter-Area Oscillation Damping*. MSc. Cairo University, Giza, Egypt, 2019.
- [19] Overschee, PV, Moor, BD. N4SID Subspace Algorithms for the Identification of Combined Deterministic-Stochastic Systems. *Automatica* 1994; 30: 75-93. DOI:10.1016/0005-1098(94)90230-5
- [20] Ljung, L. *System Identification Toolbox User's Guide*, MATLAB. Mathworks, 2012.
- [21] Kouvaritakis, B, Cannon, M. *Model Predictive Control: Classical, Robust and Stochastic*. Oxford, UK. Springer, 2016.
- [22] Ogata, K. *Discrete-Time Control Systems*. New Jersey, USA: Prentice-Hall, 1995.

APPENDIX A

Machines M2, M3 and M4 system identification and controllers data

Table 9. Machine M2 system identification and controllers data

| Machine M2                   |  |
|------------------------------|--|
| Discrete State-space Model   | $A_{M2} = \begin{bmatrix} 0 & 1 & 0 & 0 \\ 0 & 0 & 1 & 0 \\ 0 & 0 & 0 & 1 \\ 0.909 & -1.77 & -0.18 & 2.04 \end{bmatrix}$ $B_{M2} = 10^{-5} \begin{bmatrix} -0.68 \\ -3 \\ -5 \\ -7 \end{bmatrix}$ $C_{M2} = [1 \ 0 \ 0 \ 0]$ |
| Continuous Transfer Function | $tf_{M2} = \frac{-10770s - 5634}{s^4 + 11240s + 54340s^2 + 61120s + 145400}$   |
| Continuous Poles             | $P_{M2} = \{-11237, -2 + 7j, -2 - 7j, -0.24\}$   |
| State Observer Poles         | $P_{oM2} = \{0, 0.95 + 0.033j, 0.95 - 0.033j, 0.995\}$   |
| State Observer Gain          | $K_{oM2} = [-0.86 \ 0.87, -0.74, 0.76]$  |
| Min Control Horizon          | $N_{cM2} = 26$   |
| LQR Gain                     | $K_{LQRM2} = 10^4 [-1.2 \ 1.5 \ 1.3 \ -1.8]$   |

Table 10. Machine M3 system identification and controllers data

| Machine M3                   |  |
|------------------------------|--|
| Discrete State-space Model   | $A_{M3} = \begin{bmatrix} 0 & 1 & 0 & 0 \\ 0 & 0 & 1 & 0 \\ 0 & 0 & 0 & 1 \\ 0.9 & -1.7 & -0.2 & 2 \end{bmatrix}$ $B_{M3} = 10^{-4} \begin{bmatrix} -0.0631 \\ -0.2939 \\ -0.5178 \\ -0.7384 \end{bmatrix}$ $C_{M3} = [1 \ 0 \ 0 \ 0]$ |
| Continuous Transfer Function | $tf_{M3} = \frac{-9061s - 3963}{s^4 + 9719s + 44190s^2 + 424900s + 517900}$  |
| Continuous Poles             | $P_{M3} = \{-9714, -1.6 + 6.1j, -1.6 - 6.1j, -1.4\}$   |
| State Observer Poles         | $P_{oM3} = \{0, 0.97 + 0.03j, 0.97 - 0.03j, 0.97\}$  |
| State Observer Gain          | $K_{oM3} = [-0.85, 0.85, -0.72, 0.73]$   |
| Min Control Horizon          | $N_{cM3} = 5$  |
| LQR Gain                     | $K_{LQRM3} = 10^4 [-1.18 \ 1.49 \ 1.3 \ -1.8]$   |

Table 11. Machine M4 system identification and controllers data

| Machine M4                   |   |
|------------------------------|---|
| Discrete State-space Model   | $A_{M4} = \begin{bmatrix} 0 & 1 & 0 & 0 \\ 0 & 0 & 1 & 0 \\ 0 & 0 & 0 & 1 \\ -0.1 & 1.29 & -3.26 & 3.08 \end{bmatrix}$ $B_{M4} = 10^{-3} \begin{bmatrix} -0.01 \\ -0.04 \\ -0.08 \\ -0.12 \end{bmatrix}$ $C_{M4} = [1 \ 0 \ 0 \ 0]$ |
| Continuous Transfer Function | $tf_{M4} = \frac{-39.18s - 10}{s^4 + 20.51s^3 + 138.4s^2 + 798s + 206.2}$   |
| Continuous Poles             | $P_{M4} = \{-451.7, -2.17 + 6.97j, -2.17 - 6.97j, -0.27\}$  |
| State Observer Poles         | $P_{oM4} = \{0, 0.9569 + 0.03j, 0.9569 - 0.03j, 0.99\}$   |
| State Observer Gain          | $K_{oM4} = [0.17, 0.08, 0.08, 0.08]$  |
| Min Control Horizon          | $N_{cM4} = 21$  |
| LQR Gain                     | $K_{LQRM4} = 10^4 [0.12 \ -1.45 \ 3.05 \ -1.89]$  |